PB-216 861

GENERATOR FOR PRODUCING HIGH CONCENTRATIONS OF SMALL IONS

K. T. Whitby, et al

Minnesota University
Minneapolis, Minnesota

July 1960

DISTRIBUTED BY:

NTIS

National Technical Information Service
U. S. DEPARTMENT OF COMMERCE
5285 Port Royal Road, Springfield Va. 22151

only
cop

PB 216 861

Generator for Producing High Concentrations of Small Ions

LIBRARY
Environmental Protection Agency
5555 Ridge Ave., Cincinnati, O. 45213

Reprinted by

Reproduced by
NATIONAL TECHNICAL
INFORMATION SERVICE
U S Department of Commerce
Springfield VA 22151

U. S. DEPARTMENT OF HEALTH, EDUCATION, AND WELFARE

Public Health Service
Washington 25, D. C.

5

Generator for Producing High Concentrations of Small Ions

Technical Report No. 12

July 1960

Cooperative Research Project

University of Minnesota
Department of Mechanical Engineering
and
U.S. Public Health Service
(USPHS Grant No. S-23)

by
Dr. K. T. Whitby, Assistant Professor, Mechanical Engineering
A. R. McFarland, Research Fellow
D. A. Lundgren, Research Assistant

U.S. Department of Health, Education, and Welfare
Public Health Service
Division of Air Pollution
Washington 25, D.C.

Reproduced with permission from
Dr. K. T. Whitby and the University of Minnesota
by the
U.S. Department of Health, Education, and Welfare
Public Health Service

TABLE OF CONTENTS

I SUMMARY	1
II INTRODUCTION	1
III ION GENERATORS	2
A. Thermionic Generators	3
B. Ionizing Radiation	3
C. X-rays	4
D. Ultraviolet Radiation	4
E. Corona Discharge	4
F. High Frequency Electric Fields	5
IV SONIC JET ION GENERATOR	6
A. Theory	6
B. Experimental	8
1. Ionizer	8
2. Evaluation methods	10
3. Ionizer performance	12
a. Needle sharpness	14
b. Needle to orifice spacing - S	14
c. Ionizer efficiency	16
d. Ion current as a function of voltage	16
e. Ion current as a function of orifice diameter	22
V DECAY OF ION CONCENTRATION	25
A. Theory	25
1. Space charge precipitation	26
2. Recombination	28

Reproduced from best available copy.

B. Experimental 30

1. Ion concentration along the jet axis 30

2. Ion concentration perpendicular to the jet axis 34

3. Time decay of ion concentration in a room 36

REFERENCES 39

APPENDIX A. ELECTRICAL CONVERSION UNITS AND NOMENCLATURE 40

APPENDIX B. 42

Summary 42

B.1 Introduction 42

B.2 Derivation of the Governing Equation in One-Dimensional Rectangular Coordinates 44

B.3 Solution in Cylindrical Coordinates 48

B.4 Solution in Spherical Coordinates 50

B.5 Application to Unipolar Ions 51

B.6 Example: Decay of Ion Concentration in a Grounded Collector Tube 51

LIST OF TABLES AND FIGURES

TABLES

Table I Limits of variables investigated 13

FIGURES

Figure 1. Corona type free ion generators 6

Figure 2. Schematic of sonic jet ionizer field lines and streamlines 7

Figure 3. Schematic of sonic jet ionizer 9

Figure 4. Apparatus used to evaluate the unipolar ion output 11

Figure 5. Positive and negative unipolar free ion output as a function of needle to orifice spacing and voltage 15

Figure 6. Ionizer efficiency as a function of voltage and pressure 17

Figure 7. Ionizer efficiency as a function of free ion current and pressure - positive ions 18

Figure 8. Ionizer efficiency as a function of free ion current and pressure - negative ions 19

Figure 9. Free ion current as a function of voltage - positive ions 20

Figure 10. Free ion current as a function of voltage - negative ions 21

Figure 11. Air flow calibration of orifices 23

Figure 12. Unipolar free ion output as a function of air flow through the orifice 24

Figure 13. Theoretical and measured ion concentrations along the axis of the jet ionizer 32

Figure 14. Air velocities measured along the jet axis 33

Figure 15. Unipolar ion concentrations measured perpendicular to the jet axis 35

FIGURES Cont.

Figure 16. Decay of unipolar ion concentrations in a closed room 37

Figure B-1. One-dimensional rectangular system 44

I SUMMARY

A novel free ion generator capable of producing high concentrations of light ions with high efficiency has been developed. By means of a sonic orifice, ions generated in the corona about a needle point are forced through an orifice and thence free of the accelerating field. Positive and negative ion concentrations as high as 10^{11} ions/cm^3 in the sonic jet have been produced. Ion outputs of 10^{14} per sec. using about 2.5 cfm of free air at 30 psig through a 1/16 inch orifice have been achieved. The generator is capable of producing positive, negative or an equal mixture of positive and negative ions.

The high ion concentrations produced by this generator decay very rapidly due to space charge and recombination effects. To better understand these phenomena a theoretical and preliminary experimental study of ion decay has been made. These studies show that the ion concentration drops off approximately as the second power of the distance from the generator along the axis of the jet. Concentrations five feet from the ionizer along the jet axis are on the order of 10^6 ions/cm^3.

II INTRODUCTION

During the course of development of a generator for making homogenous aerosols from methylene blue by the evapora-

tion of alcohol or water solutions of the dye, it was found that the generated particles were highly charged under certain conditions. It was eventually found that the only practical method for neutralizing these particle charges was by mixing the particles with a high concentration of mixed positive and negative small ions.

This report describes the ion generator used to neutralize these particle charges. Since the ion generator is believed capable of producing free ion concentrations several orders of magnitude above currently available generators, it is reported separately from the aerosol generation work. Evaluation of this device has only been partial because ion generation is outside the main stream of research conducted at the particle technology laboratory, and because adequate instrumentation is not available. Nevertheless it is believed that data presented here is complete enough to outline essential characteristics of this device.

III ION GENERATORS

Free small ions at atmospheric pressure may be produced by the following methods: (1)

Thermionic ion generation (hot wires)

Ionizing radiation (radioactive materials)

X-Rays

Ultraviolet photo ionization

Corona discharge

High frequency electric fields

Performance and general characteristics of the generators are given below.

A. Thermionic Generators

Ions are produced by a hot surface, usually metal, and separated as to desired polarity by an electrical field of several hundred volts. Martin (1) describes an experimental generator capable of producing total ion currents of about 10^{-6} amps. The usable ion current would probably be less than this due to the difficulty of removing the ions from the generator. Principal disadvantages of the thermionic generator are its short life and its heating of the gas to be ionized.

B. Ionizing Radiation

A convenient method for making ions free from any contaminating ozone and oxides of nitrogen is by the use of ionizing radiation. Martin (2) and Hicks and Beckett (3) describe generators using Polonium 210. Alpha particles emitted by the radioactive source produce a mixture of positive and negative ions up to about 4 cm. from the source. Ions of the desired sign are then separated by an electric field on the order of a hundred volts and, or by a flow of air through the ionizing zone.

Martin (2) states that a 200 micro-curie source of polonium will produce about 1.2×10^{10} ions per second.

The disadvantages of this type of ion generator are the cost and health hazard involved in preparing the fairly intense radioactive sources required to generate high ion concentrations.

C. X-rays

X-rays are not a satisfactory source of ions for general laboratory work because of the hazard and cost of equipment necessary to generate high ion concentrations.

D. Ultraviolet Radiation

Only relatively low concentrations of ions are produced by ultraviolet radiation. Ultraviolet light of the intensity to produce ions also produces considerable quantities of ozone. For these reasons ultraviolet is not a satisfactory method for generating ions.

E. Corona Discharge

A high voltage (2000 volts and up) corona discharge from a point or fine wire is a simple and inexpensive source of large quantities of gas ions. Corona ionizers are widely used for charging particles in electrostatic air cleaners. Yaglou et al. (4) state that they were

able to produce ion concentrations of about 10^6 ions/cm^3 in the breathing zone of subjects using a corona ionizer.

The principal problem in designing a corona ionizer to produce free ions is to find a means for removing the ions from the strong electric field necessary to sustain the corona discharge. About the minimum practical starting voltage for a corona discharge is 3000 volts across a gap of several millimeters. Since the mobility of small ions is between 1 and 2 cm/sec. per volt/cm., it is apparent that the ions will be traveling a substantial fraction of the speed of sound and that in the usual electrostatic air cleaner type ionizer, the same electric field which generates the ions will also collect most of them. Because of their inefficiencies, corona ionizers for producing free ions have tended to be large and to require relatively high currents (milliamperes) to produce even moderate free ion concentrations. These high currents may produce an undesirable amount of ozone and oxides of nitrogen. The corona ionizer described in this report overcomes most of the difficulties by using a sonic orifice to force up to 100% of the ions produced in the corona through the orifice and hence free of the electric field.

F. High Frequency Electric Fields

Francis (5) reports that very high concentrations of free ions can be produced by high frequency electric fields.

However, the cost and complexity of the microwave equipment required limits its usefulness for most laboratory purposes.

IV SONIC JET ION GENERATOR

A. Theory

Corona type free ion generators all use air streams to separate the ions from the electrostatic field. Typical arrangements are shown in Figure 1.

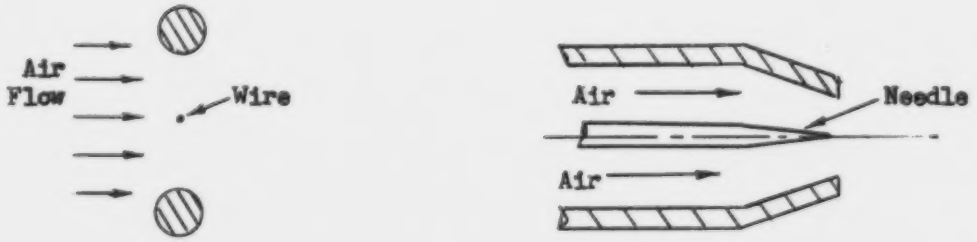

(a) Wire Type (b) Jet Type

Figure 1 Corona type free ion generators.

Figure 1(a) illustrates the common wire and bar ionizers. At practical wire voltages (5 to 30 KV) and practical air velocities (10 to 100 ft/sec.) only a small fraction of 1% of the ions generated will escape the electric field.

Figure 1(b) illustrates a commerical ionizing gun which generates the ions with a corona at the tip of a

needle. Again the efficiency is low at the voltages and air velocities used.

Since the average velocity of the ions cannot exceed the local velocity of sound, increasing the air velocity through the ionizers of Figures 1(a) and 1(b) would increase their efficiency. However, to achieve sonic velocity with either of these designs would require an impractical amount of power.

The sonic jet ionizer achieves high efficiency with relatively small quantities of compressed air by using the arrangement of Figure 2.

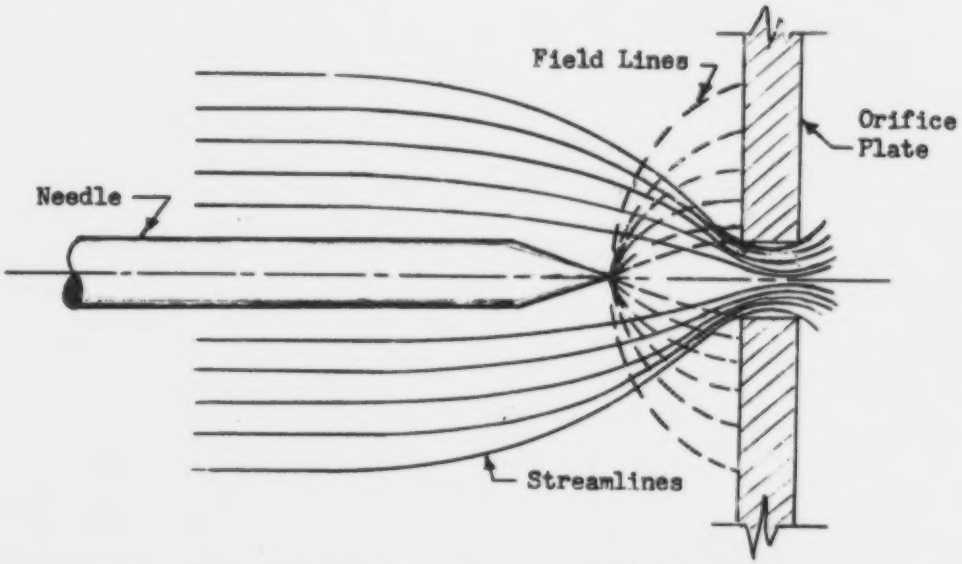

Figure 2 Schematic of sonic jet ionizer field lines and streamlines

Ions generated in the corona at the tip of the needle would normally travel along the field lines to

the orifice plate. Their velocities will be highest on the lines closest to the orifice axis and lowest on lines farthest from the orifice. However, if the gas is flowing through the orifice at sonic velocity the inward component of velocity from the "sink" flow of the fluid may cancel the outward component of the "source" flow of the ions.

Several combinations of the orifice diameter and spacing, needle voltage and air pressure have been found experimentally at which 100% efficient conversion of corona current into free ions have been obtained.

B. Experimental

1. Ionizer A schematic of the ionizer used to obtain the data of this report is shown in Figure 3. A 1.5 inch ID lucite tube A is threaded at each end to receive end caps B and C. End cap B has a hole and thumb screw for retaining the needle and a 1/4 inch copper tube compressed air connection H. End cap C is recessed to hold the orifice plate D accurately centered. Needle positioning bracket E is made from 1/4 inch lucite and serves to center the needle F accurately in the center of the orifice. The holes for the two screws holding bracket E to the orifice plate D are made large so that the bracket may be adjusted to center the needle in the hole. This is most conveniently done by

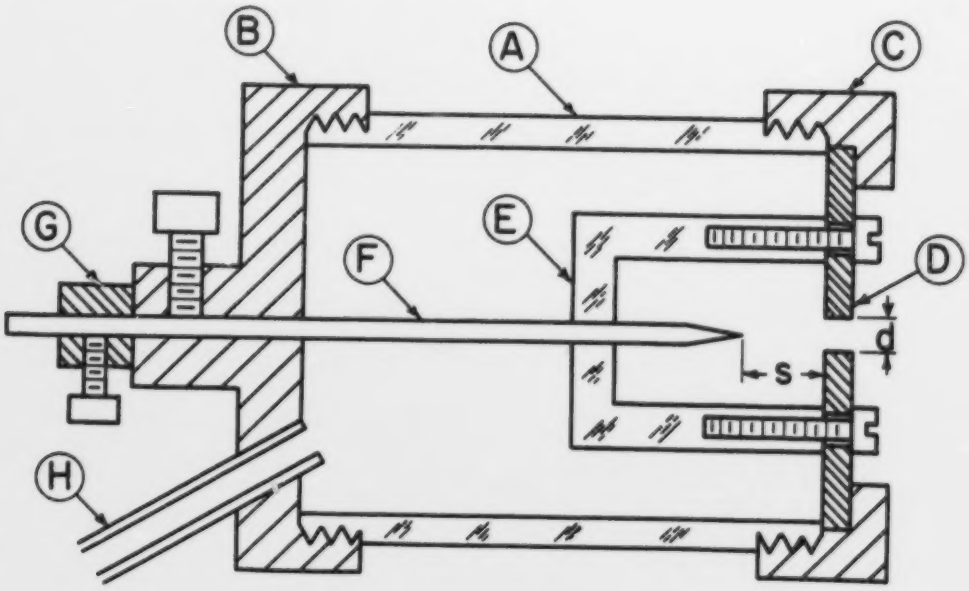

d — Orifice diameter
s — Needle spacing
A — Lucite tube
B — End cap
C — End cap
D — Orifice plate
E — Needle positioning bracket
F — Needle
G — Needle stop
H — Air connection

Figure 3 Schematic of sonic jet ionizer

loosening the screws, pushing the needle forward until it protrudes through the hole and then tightening the screws.

The needle spacing S was set with the aid of a small jig made by glueing spacers of the required thickness to flat glass plates. With the cap C and orifice plate D removed, the end of the tube A is set on the glass plate and the needle dropped down onto the spacer. Stop G is then tightened so that the needle may be removed for inspection without changing the spacing S.

By experiment it was found that the needle tip had to be sharpened to less than 0.001 inch diameter for satisfactory operation at the lowest voltage. The radius may be somewhat larger at voltages above 5 KV, although the highest ion currents can only be obtained with 0.001 inch or smaller tip diameter. The 1/16 inch piano wire used in the original ionizer is probably not the best material since it had to be sharpened after several hours of operation.

2. Evaluation methods Two general types of evaluation of the ionizer were made. First, the total ion current output as a function of needle spacing, orifice diameter, pressure, needle voltage, etc. were made using the arrangement shown in Figure 4. Power was supplied to the ionizer from a standard ungrounded high voltage D.C. power supply or from an alternating current transformer.

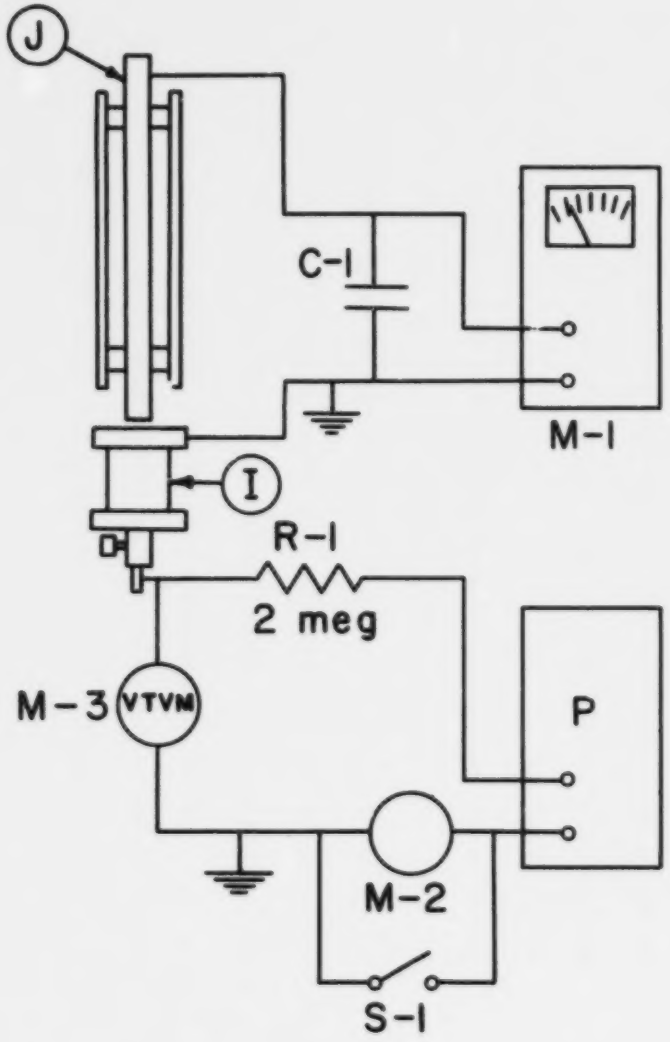

P = 20 KV power supply
M-1 = Keithley 610A electrometer
M-2 = 50 microampere meter
M-3 = VTVM with HV probe
R-1 = 2 meg, 1 watt resistor
C-1 = 0.03 μF low leakage capacitor
S-1 = Micro switch to protect meter
(I) = Ionizer
(J) = 2 cm ID by 60 cm copper tube

Figure 4 Apparatus used to evaluate the unipolar ion output

D.C. current supplied to the needle was measured with a microammeter. Corona and power supply leakage currents determined with the needle retracted were subtracted from the needle corona currents.

Total free ion current was measured by directing the jet of ions and air into a carefully insulated copper tube 2 cm. ID and 60 cm. long. This tube was connected to a Keithley model 610A electrometer used as a micro-micro-ammeter. Capacitor C-1 was used to damp the electrometer. Calculations using the space charge theory of appendix B showed that at least 99% of the ions leaving the ionizer would precipitate within the tube due to the space charge effect. Some estimate of the high electric fields formed by the high ion output of this generator can be had from the fact that potentials of as high as 25,000 volts were observed when the tube was left ungrounded and the voltage on the ionizer needle was 5000 volts.

The second type of evaluation made was to determine the ion concentration both along the ionizer jet and perpendicular to it. A limited number of measurements of the decay rate of positive and negative ions in a small room were also made. These are described in Section V.

3. Ionizer Performance Using the apparatus shown in Figure 4 the following variables were investigated over the range indicated. This does not imply that the ionizer

will not work satisfactorily beyond the limits given. These limits were determined by the existing laboratory equipment and time.

Table I

Limits of Variables Investigated

Variable	Range
Pressure	0-50 psig
Voltage	0-9000 volts
Orifice dia. = d	1/64 to 1/16 inch
Needle spacing = S	0.62 to 6.4 mm.
Ions	(+), (-) and 1/2 (+) and 1/2 (-)
Ionized gas	air
Maximum free ion current	0-15 micro-ampere = 0-9 x 10^{13} ions/sec

From preliminary experiments it was discovered that the smallest practical spacing, S, was about 0.5 mm. At smaller needle to orifice spacings, sparking occurred before a stable corona was started. It was also discovered that the efficiency did indeed approach 100% above the critical pressure ratio, where efficiency is defined by equation 1.

$$\eta = \text{efficiency} = \frac{\text{free ion current}}{\text{corona current}} \qquad (1)$$

It was also determined that operation at a pressure of 30 psig using a 1/16 inch orifice was quite satisfactory and also produced ions in about the quantity desired. Therefore the effects of needle spacing and ion decay were investigated at this condition.

Since A.C. microammeters were not available, most of the ionizer evaluations were made using either (+) or (-) D.C. on the needle. Some ion decay experiments were made with A.C. on the needle.

Results of the various experiments are discussed below.

a. Needle sharpness It was determined that ion currents were not reproducible at the lower voltages if the tip diameter was greater than about 0.001 inch. The needle had to be resharpened every time a spark occurred because even the weak spark permitted by the 2 meg current limiting resistor burned the needle tip to a greater radius. However, tip radius would not be of such critical importance for most applications because the ionizer will still produce approximately 70% of the maximum sharp needle output after sparking if the voltage is 5 KV or above.

b. Needle to orifice spacing - S Free ion current output at 30 psig pressure using a 1/16 inch orifice (1.59mm) for needle to orifice spacings from 0.62 to 6.4 mm. are given in Figure 5. Corona starting voltages are the intercepts of the curves with the zero current axis. As would be expected negative corona starting voltages are lower than positive. Arcing voltages are given by the circles surrounding the X's . Even though very high free ion currents were obtained at the 0.62 mm.

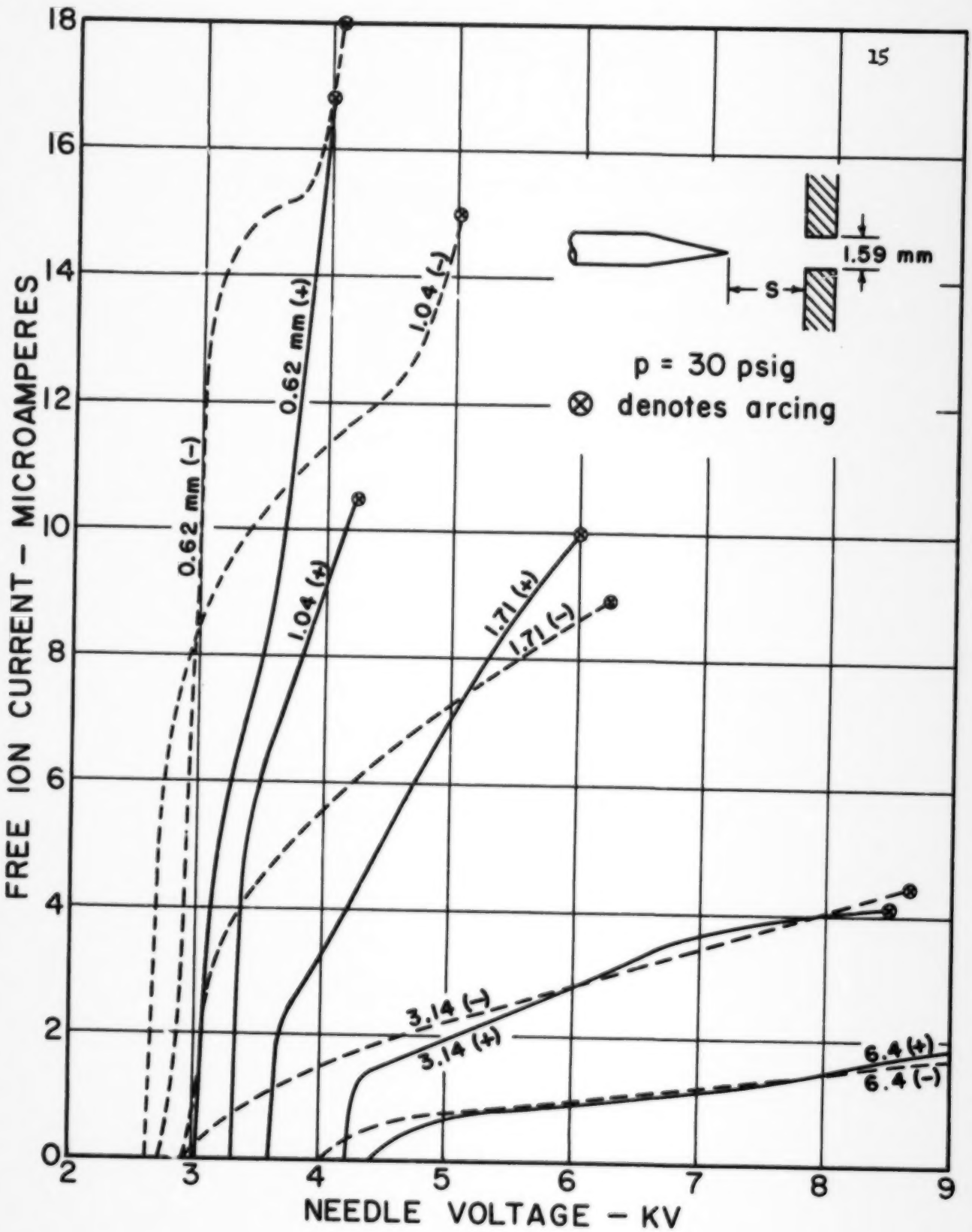

Figure 5 Positive and negative unipolar free ion output as a function of needle to orifice spacing and voltage

spacing, the voltage range for satisfactory operation is too narrow to be of practical value. Best operation appears to be in the 1.5 to 3 mm. range.

c. Ionizer efficiency Ionizer efficiency as a function of (-) needle voltage is plotted in Figure 6 for various pressures. It will be noted that 100% efficiencies are only achieved at pressures above critical.

Efficiency is plotted against free ion current in Figures 7 and 8. It will be noted that efficiency drops off at high currents due to leakage of ions to the orifice plate.

These data show that it is possible to obtain 100% efficiency. For most applications of the ionizer, stability and the absolute magnitude of the free ion current are more important than the efficiency as long as the efficiency is relatively high. Although no ozone measuring equipment was available, ozone production is believed to be quite low relative to the ion output. The odor of ozone was detected only at conditions near sparking where the corona current was high and the efficiency low.

d. Ion current as a function of voltage Ion current as a function of voltage for various pressures and a spacing of 1.71 mm. is shown in Figures 9 and 10. Note much higher free ion currents can be obtained at pressures above critical. Also the higher arcing voltages

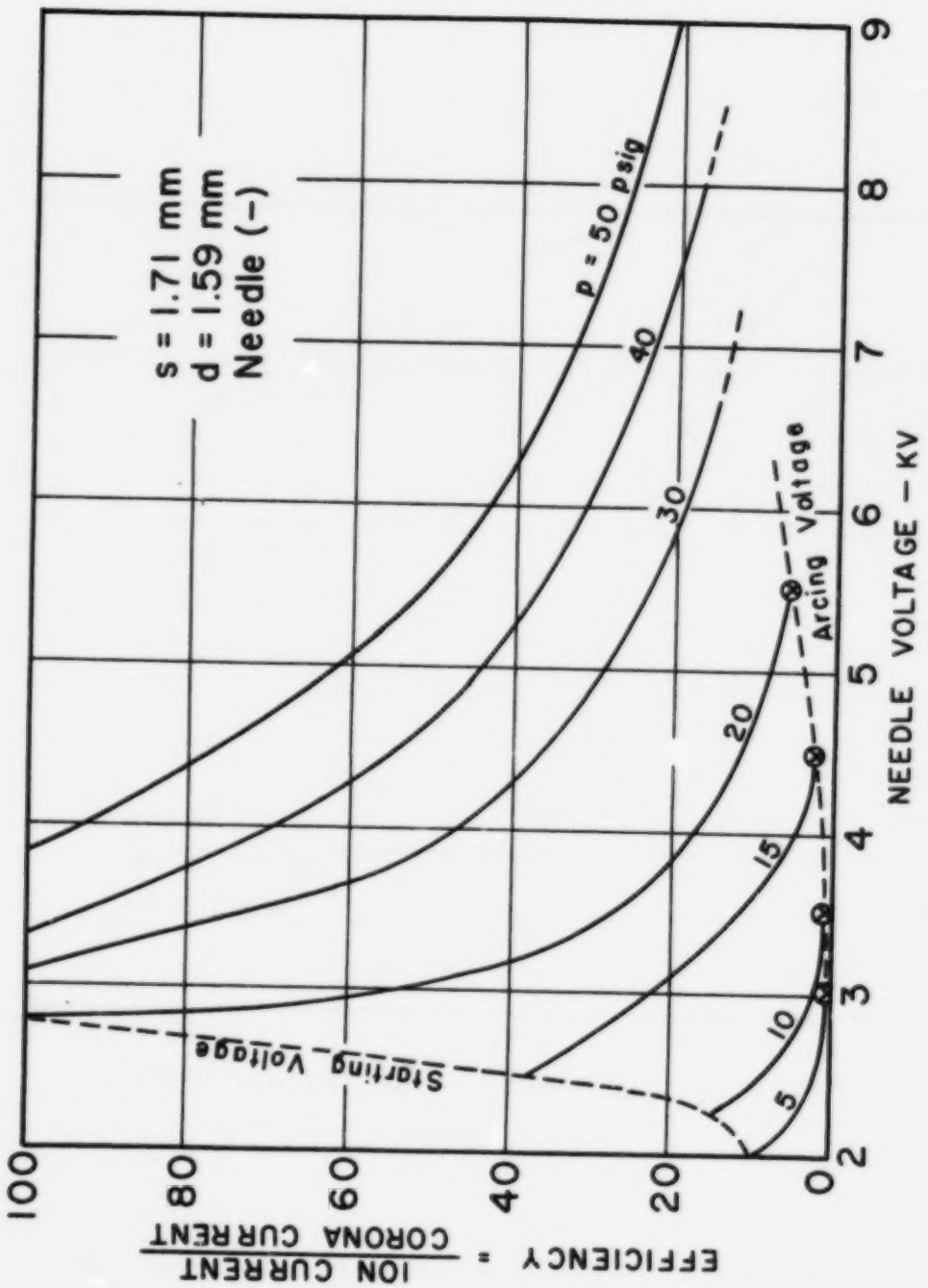

Figure 6 Ioniser efficiency as a function of voltage and pressure

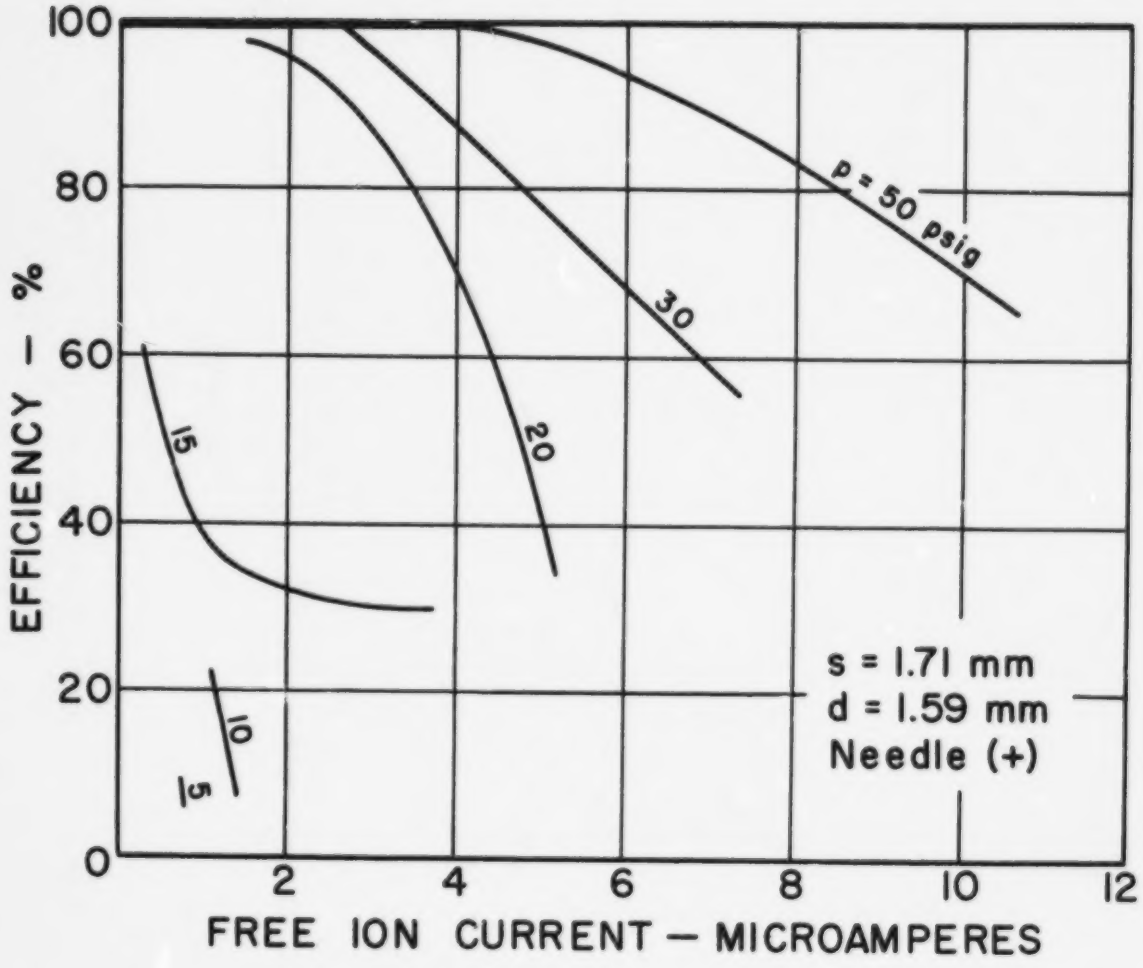

Figure 7 Ioniser efficiency as a function of free ion current and pressure - positive ions

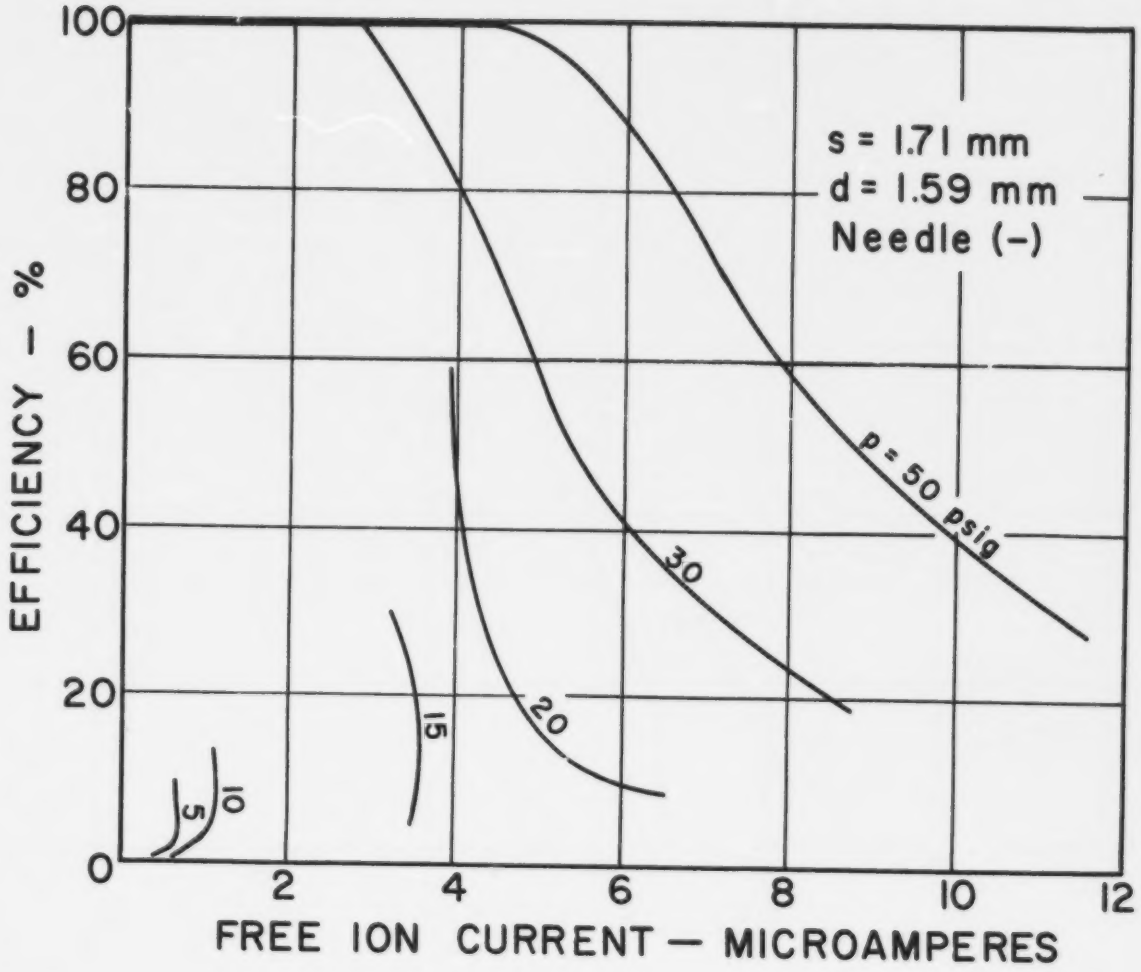

Figure 8 Ionizer efficiency as a function of free ion current and pressure - negative ions

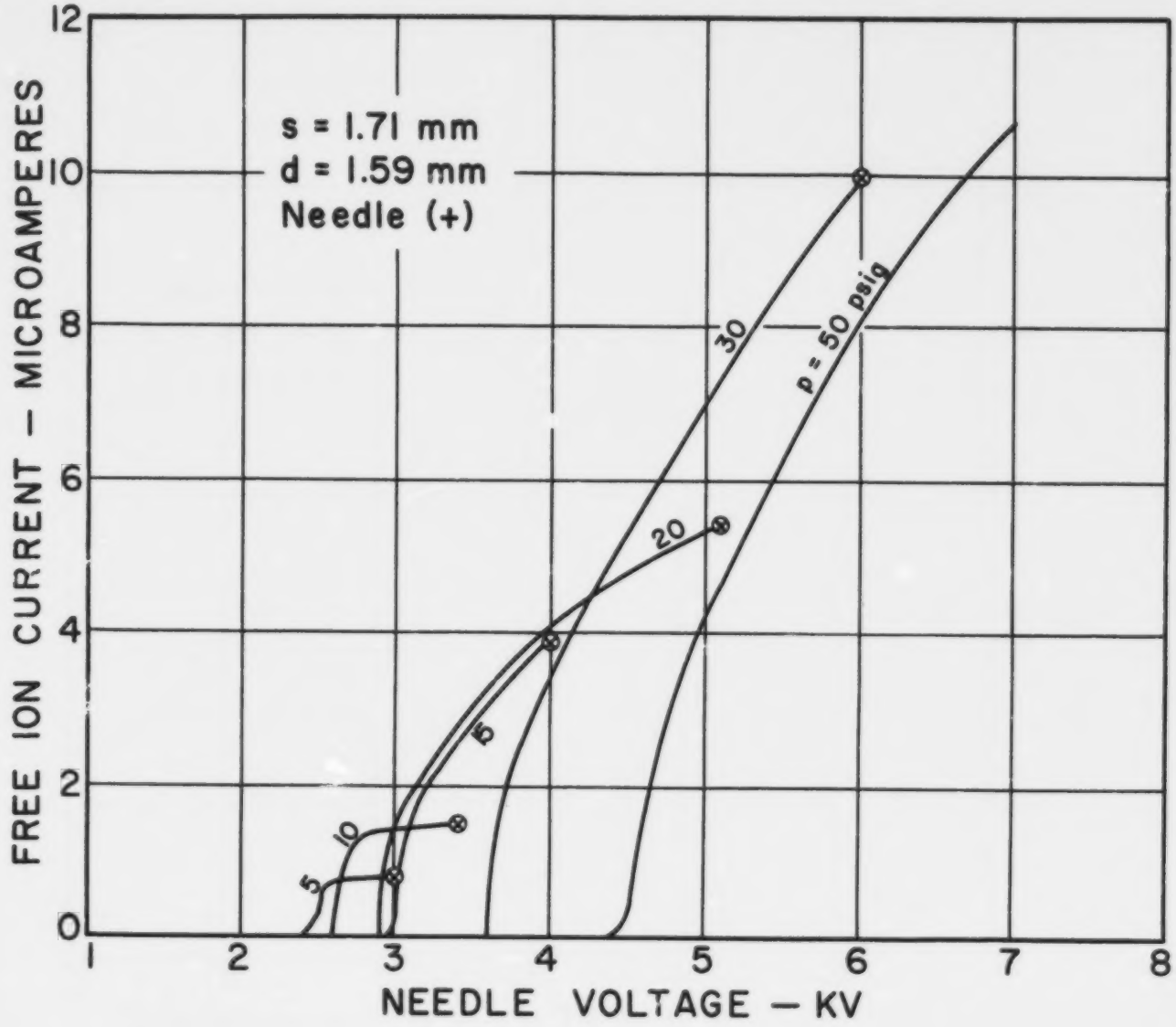

Figure 9 Free ion current as a function of voltage - positive ions

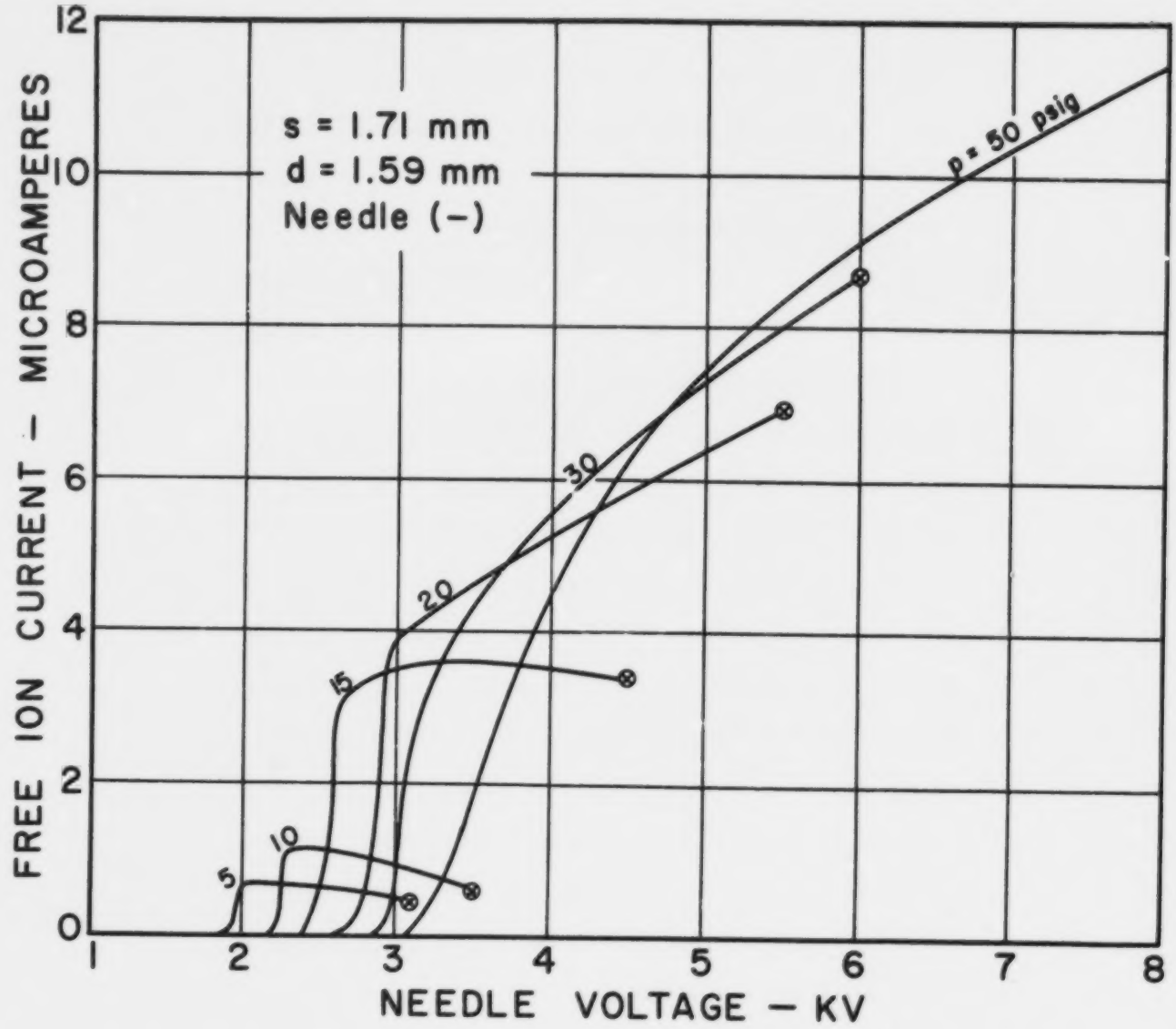

Figure 10 Free ion current as a function of voltage - negative ions

permit higher operating voltages and less sensitivity to needle tip radius.

From Figure 10 it will be noted that the negative free ion current reaches a peak and then drops off as the needle voltage is increased for pressures below critical. The reason for this is not known.

e. Ion current as a function of orifice diameter

The effect of orifice diameter was investigated over a limited range. Of particular interest were very small orifices that would only allow small air flows. The air flow calibrations of the three orifices used are shown in Figure 11. The 1/64 inch orifice used requires only 0.14 cfm of free air at 30 psig. Free ion currents as a function of orifice air flow is shown in Figure 12. Note that the free ion current for this condition is almost directly proportional to the free air flow and hence to the mass flow through the orifice. Further it is seen that a free ion current of 0.31 micro-amperes is obtained with the 1/64 inch orifice corresponding to 1.9×10^{12} ions per second. This is still a relatively strong ion source. Operation of the ionizer using a small orifice would be desirable whenever the noise from the larger orifice would be objectionable or only a small volume of compressed air is available.

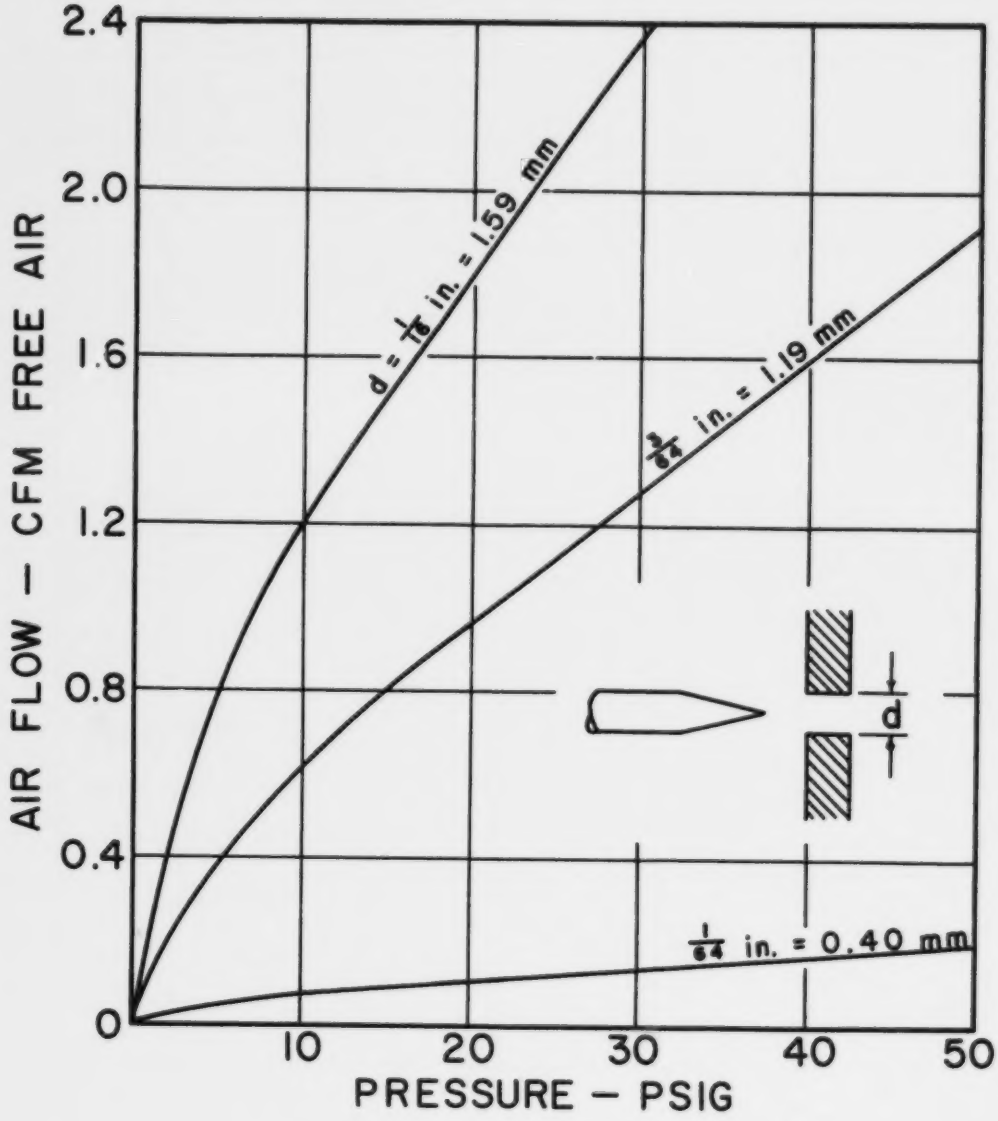

Figure 11 Air flow calibration of orifices

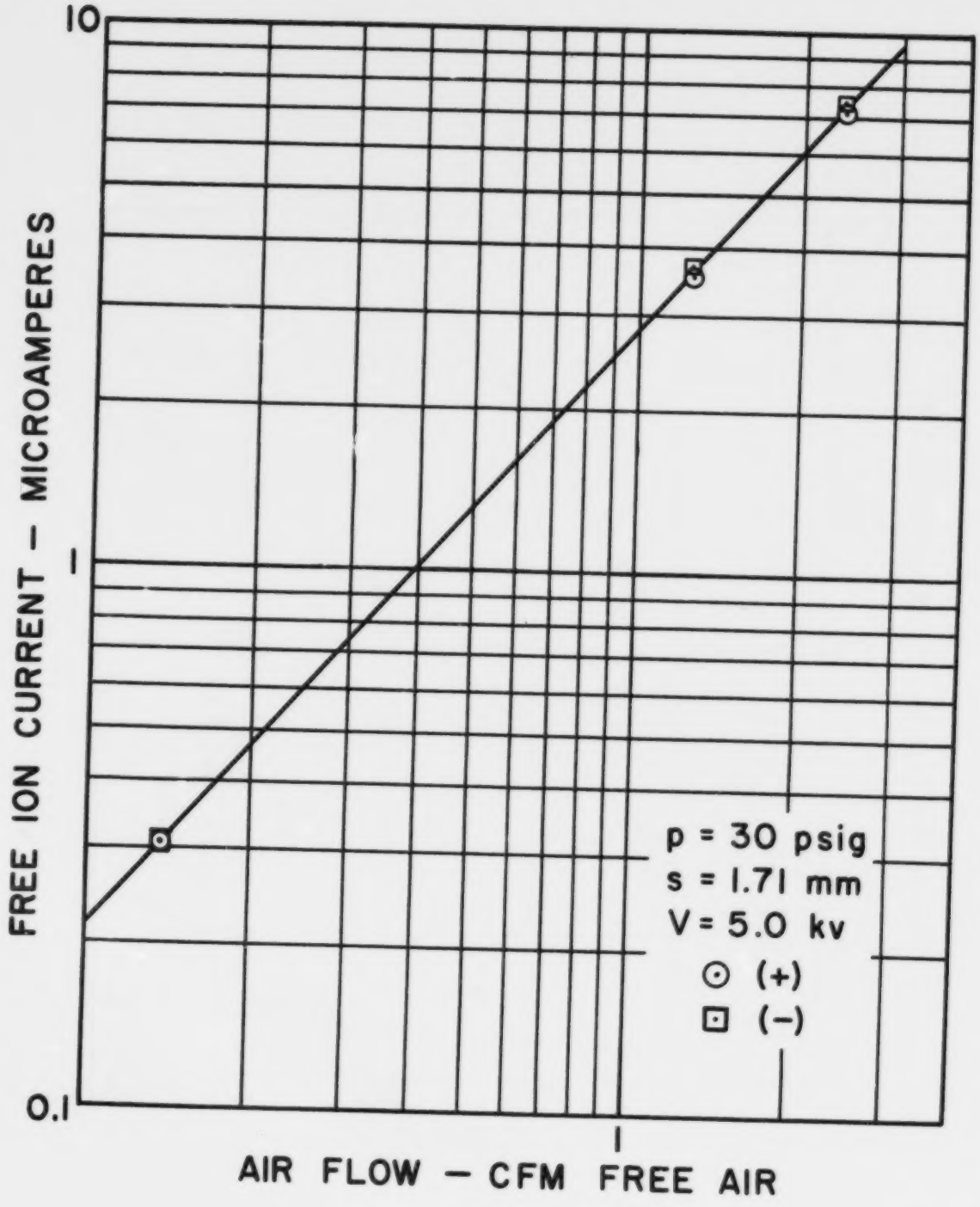

Figure 12 Unipolar free ion output as a function of air flow through the orifice

V DECAY OF ION CONCENTRATION

A. Theory

Any application of a strong ion source such as the sonic jet generator requires a knowledge of the decay processes in order to predict the ion concentration as a function of time or as a function of distance from the generator. The high ion concentration leaving the generator decays very rapidly. For example if the concentration leaving the ionizer is 4.2×10^{10} ions/c.c., the concentration will drop one order of magnitude to 4.2×10^{9} ions/c.c. in only 60 micro-seconds due to space charge precipitation when generating unipolar ions or by recombination when generating a mixture of (+) and (-) ions.

Several processes cause the decay of ion concentrations. Unipolar ion concentrations decay due to space charge precipitation on the surroundings and combination with particles or condensation nuclii. For mixed (+) and (-) ions these are space charge precipitation (if the number of (+) and (-) are not equal) and recombination of the various sizes of ions and particles. For strong ion sources the two important decay mechanisms are undoubtedly space charge precipitation for unipolar ions and recombination for mixed ions. Even though the generator may generate unequal numbers of (+) and (-) ions, decay and recombination very rapidly equalizes the number of ions

so that measurements at practical distances from the ionizer always show nearly equal concentrations.

1. Space charge precipitation In any closed volume containing unipolar charged particles or ions, the particles or ions will migrate to the walls due to the electric field caused by the space charge. The dynamics of such a space charge in the presence of an electric field has been known for a long time due to its importance in electron tubes and other electronic applications.

Less work has been done on space charges in the absence of external fields. Wilson ( ) has derived equations giving the time rate of deposition of charged aerosol particles in the absence of any fields assuming that the concentration of charged particles is constant in a radial direction. Foster (8) extended Wilson's derivation to moving clouds.

Recently one of the authors (McFarland) derived Wilson's equations by a more rigorous treatment and showed that the radial concentration is indeed constant. His derivation is given in Appendix B.

From equation B-30 Appendix B, the ion concentration in an enclosed volume as a function of time is given by:

$$n = \frac{n_o}{4 \pi n_o e Z t + 1} \qquad (2)$$

where:

n = number concentration of ions - ions/cm^3

n_o = initial concentration at $t = 0$

e = electron charge - 4.8×10^{-10} stat coulomb

Z = ion mobility - cm/sec per stat volt/cm

t = time - sec.

From equation 2 it is noted that ion concentration due to space charge precipitation is independent of the dimensions and hence independent of geometry of the volume. Physically this can be explained by the fact that for a given concentration the increased rate of precipitation caused by the increased field of a larger volume is exactly compensated for by the greater distance the ions must travel.

The unipolar ion concentration along the axis of a jet of ions and air discharging from an ionizer may be calculated if the following assumptions are made:

(a) Ion concentration is a function only of the time since a given volume of gas left the ionizer.

(b) Velocity along the jet axis is given by:

$$U = \frac{b}{x} \qquad (3)$$

where:

U = velocity along jet axis - cm/sec

b = a constant - $\frac{cm^2}{sec}$

x = distance from jet - cm.

Reproduced from best available copy.

now:

$$t = \int_0^x \frac{dx}{U} = \int_0^x \frac{x\,dx}{b} = \frac{x^2}{2b} \qquad (4)$$

Substituting equation 4 into equation 2 gives:

$$n = \frac{n_o}{\frac{4\pi n_o e Z x^2}{2b} + 1} \qquad (5)$$

The constant b may be determined from equation 3 by measuring the velocity along the jet axis. If b, Z, and n_o are known it is possible to calculate the concentration at any distance from the ionizer. Some comparisons of calculations and experimental measurements are given below in Section V. B.1.

2. Recombination When alternating current is applied to the needle the ionizer will generate (+) ions on the positive half of the cycle and negative ions on the other half. These ions will mix a few cm. outside of the ionizer due to turbulent mixing and space charge effects. Beyond a few cm. from the ionizer the ions may be treated as a mixture of positive and negative ions. Since the ions are generated in approximately equal quantities, the space charge will be essentially zero and the concentration decays primarily by recombination.

The recombination rate is given by:

$$\frac{dn}{dt} = q - \alpha n^+ n^- \qquad (6)$$

where:

q = rate of generation - ions/cm^3 per sec.

α = recombination coefficient = cm^3/sec.

n^+ and n^- are the ion concentrations - ions/cm^3

In the ion jet q = 0 and $n^+ = n^- = n$, therefore:

$$\frac{dn}{dt} = - \alpha n^2$$

Integrating from $t = 0$ to t and n_o to n yields

$$\frac{1}{n} - \frac{1}{n_o} = \alpha t \qquad (8)$$

or:

$$n = \frac{n_o}{\alpha n_o t + 1} \qquad (9)$$

If equation 4 is substituted in equation 9 the concentration along the jet axis is:

$$n = \frac{n_o}{\frac{\alpha n_o x^2}{2b} + 1} \qquad (10)$$

A comparison of equation 2 and 5 with 9 and 10 respectively shows that the form of the decay is the same whether the mechanism is space charge precipitation or recombination. Furthermore if it is assumed that each ion has one charge and appropriate values of Z, e and α are substituted into equation 2 and 9 (i.e. $e = 4.8 \times 10^{-10}$ stat coulomb, $Z = 600$ cm/sec per stat volt/cm and $\alpha = 1.6 \times 10^{-6}$ cm^3/sec) equation 2 for space charge precipitation becomes:

$$n = \frac{n_o}{3.61 \times 10^{-6} n_o t + 1} \qquad (11)$$

and equation 9 for recombination becomes:

$$n = \frac{n_o}{1.6 \times 10^{-6} n_o t + 1} \qquad (12)$$

Two things are apparent from a comparison of equations 11 and 12. First, the rate of decay due to space charge or recombination is nearly the same. Second, for a strong source of ions such as the jet ionizer, ($n_o = 10^{10}$ ions/c.c.) the ion concentration as a function of time or as a function

of distance from the generator is going to be independent of the initial concentration n_o after a few milliseconds or beyond a few cm. distance from the ionizer. Thus for large n_o , equations 2 and 5 and 9 and 10 become

For space charge precipitation:

$$n = \frac{1}{4\pi e Z t} \qquad (13)$$

$$n = \frac{2b}{4\pi e Z x^2} \qquad (14)$$

For recombination:

$$n = \frac{1}{\alpha t} \qquad (15)$$

$$n = \frac{2b}{\alpha x^2} \qquad (16)$$

The above equations may be used to calculate the ion concentration at various distances from the ionizer.

B. Experimental

Several different kinds of decay measurements were made. The results of these measurements and comparisons with the theory are given below.

1. Ion concentration on the jet axis. The ion generator was set up in a room 3 feet from the floor so that the jet projected horizontally. Ion concentration was then measured along the jet axis from about 15 to 700 cm. Concentration could not be measured closer than 15 cm. due to the large size of the ion counter available (8 by 9 cm. inlet).

Ion concentration was measured using a Wesix Electric Mark IV Ion Collector (6) connected to the Keithley 610 A electrometer. The ion collector was operated at 200 volts and 15 cfm. At this condition all ions with mobilities greater than 0.007 cm/sec per volt/cm are collected. At ion concentration above about 10^5 ions/cm^3 the potential gradient due to space charge of the dominant ion polarity was large enough so that only the concentration of the predominant ion polarity could be measured. However, no difficulty was experienced in measuring both positive and negative ion concentrations when the generator was discharging approximately equal quantities of ions of each sign. Under these conditions the net space charge is essentially zero and the 200 volt potential on the plates of the ion counter is sufficient to precipitate the ions. At unipolar ion concentrations above about 10^5 per cm^3 the space charge will precipitate approximately one half of the ions on the collector plates and one half on the charged plates. Therefore the observed ion current must be doubled in order to calculate the true ion concentration.

Positive, negative and mixed ion concentration at various distances are plotted in Figure 13 over the range from 15 to 600 cm. Also shown are the theoretical curves. The constant b was determined from equation 3 by measuring the velocity with a Hastings precision air meter and plotting the velocity versus 1/x as in Figure 14.

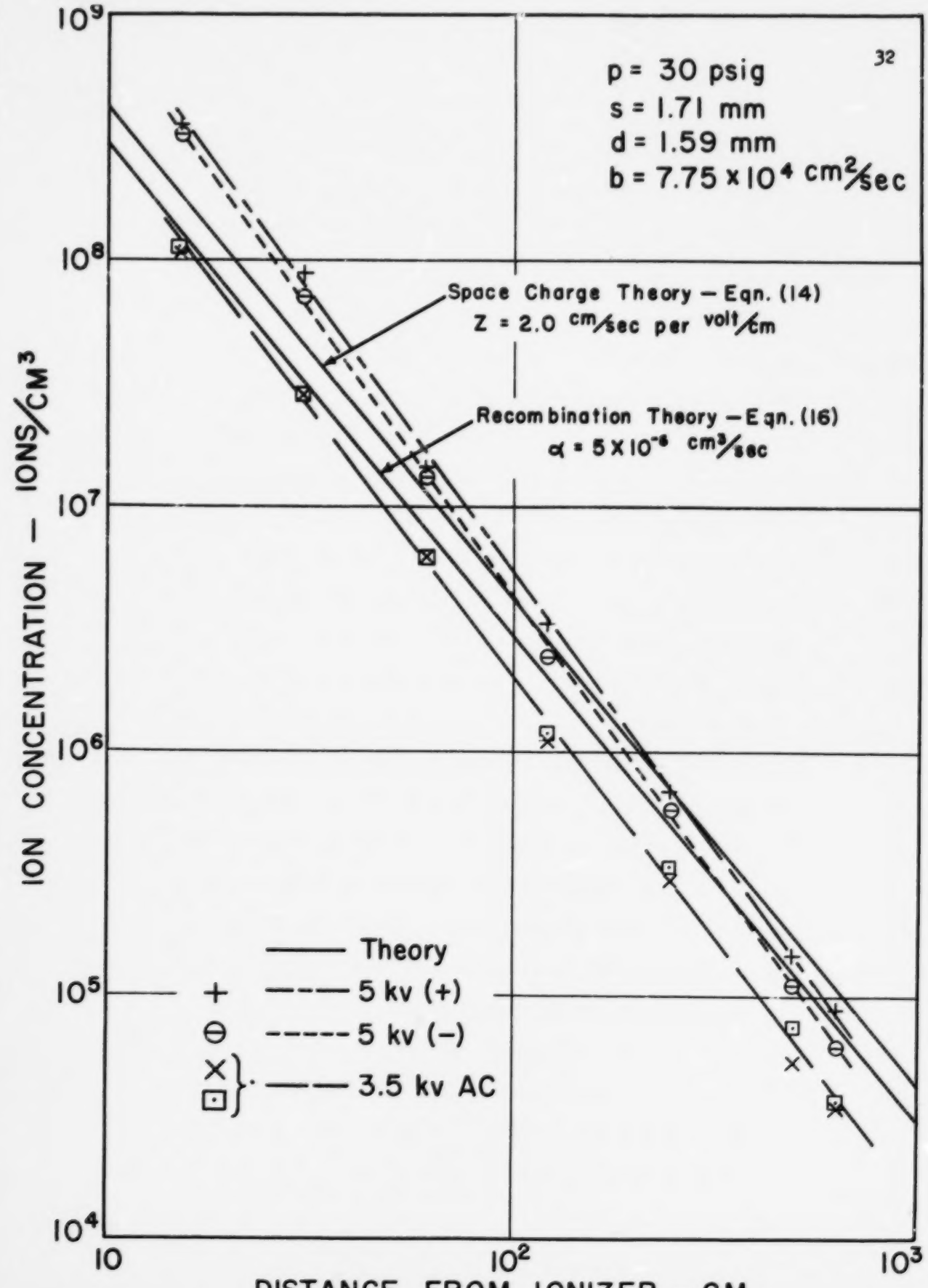

Figure 13 Theoretical and measured ion concentrations along the axis of the jet ionizer

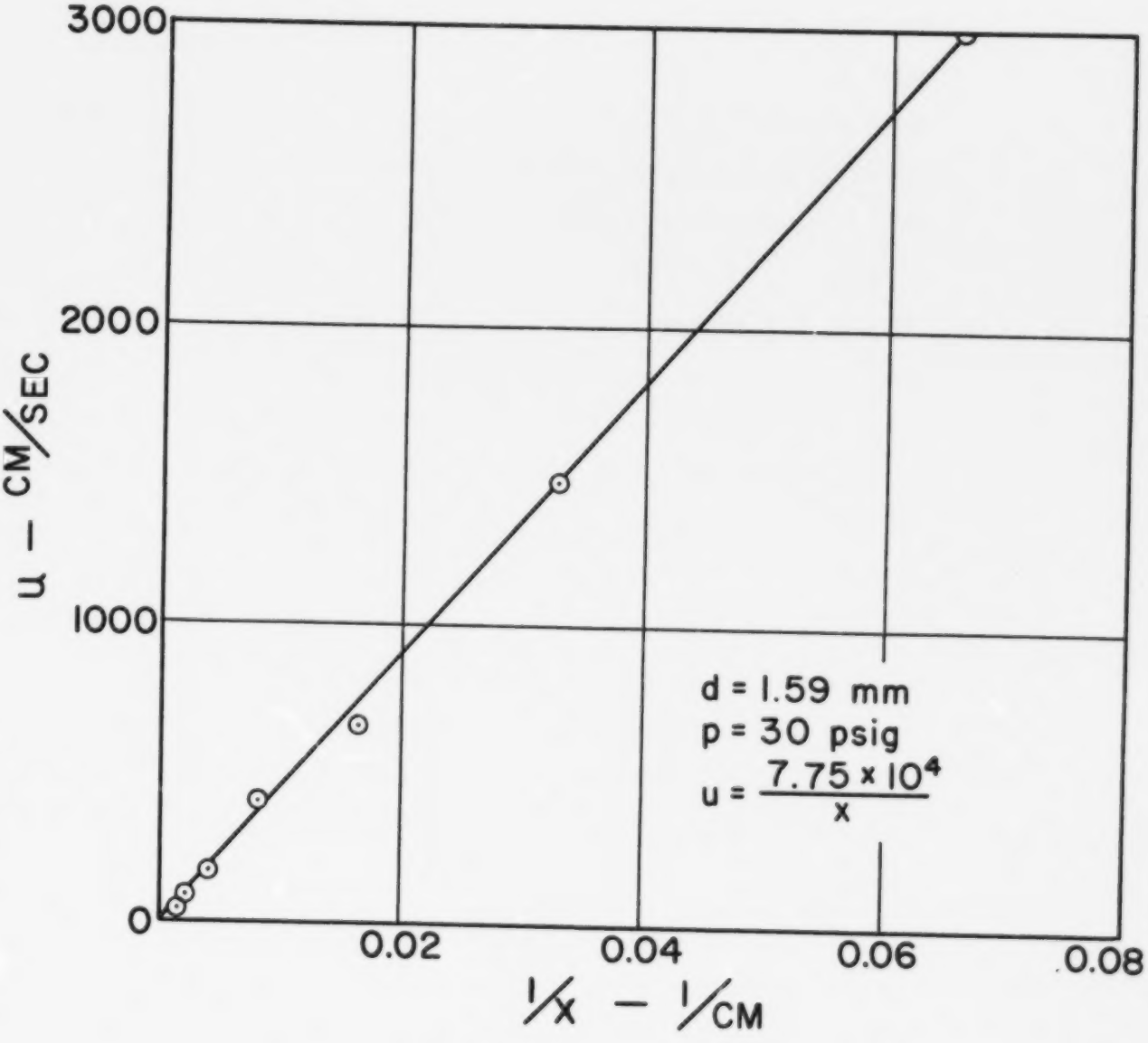

Figure 14 Air velocities measured along the jet axis

The theoretical curve for space charge decay was then calculated from equation 14 and that for recombination from equation 16. From Figure 13 it can be seen that the experimental measurements with unipolar small ions agree quite well with the theory using the accepted value of the mobility of 2 cm/sec per volt/cm. However, the position of the recombination theory line for an $\alpha = 5 \times 10^{-6}$ cm^3/sec, relative to the decay curve for the (+) and (-) ion mixture, indicates that either the recombination coefficient is much higher than the accepted value of 1.6×10^{-6} for small ions (9), or that there is some unknown error in the measurements. It is possible that the recombination coefficient is higher at high ion concentrations shortly after the ions have been generated, and before the small ions have had much opportunity to grow in size. Most of the accepted values for the recombination coefficients have been determined at low concentrations and under equilibrium conditions where the small ions have existed for much longer times than were used here.

2. Ion concentration perpendicular to the jet axis. The jet ionizer was set up in the center of a closed room 14.6 x 15.8 x 8.7 feet, with the jet directed upward as shown in Figure 15. Ion concentration was then measured from 30 to 200 cm. in a plane perpendicular to the jet axis.

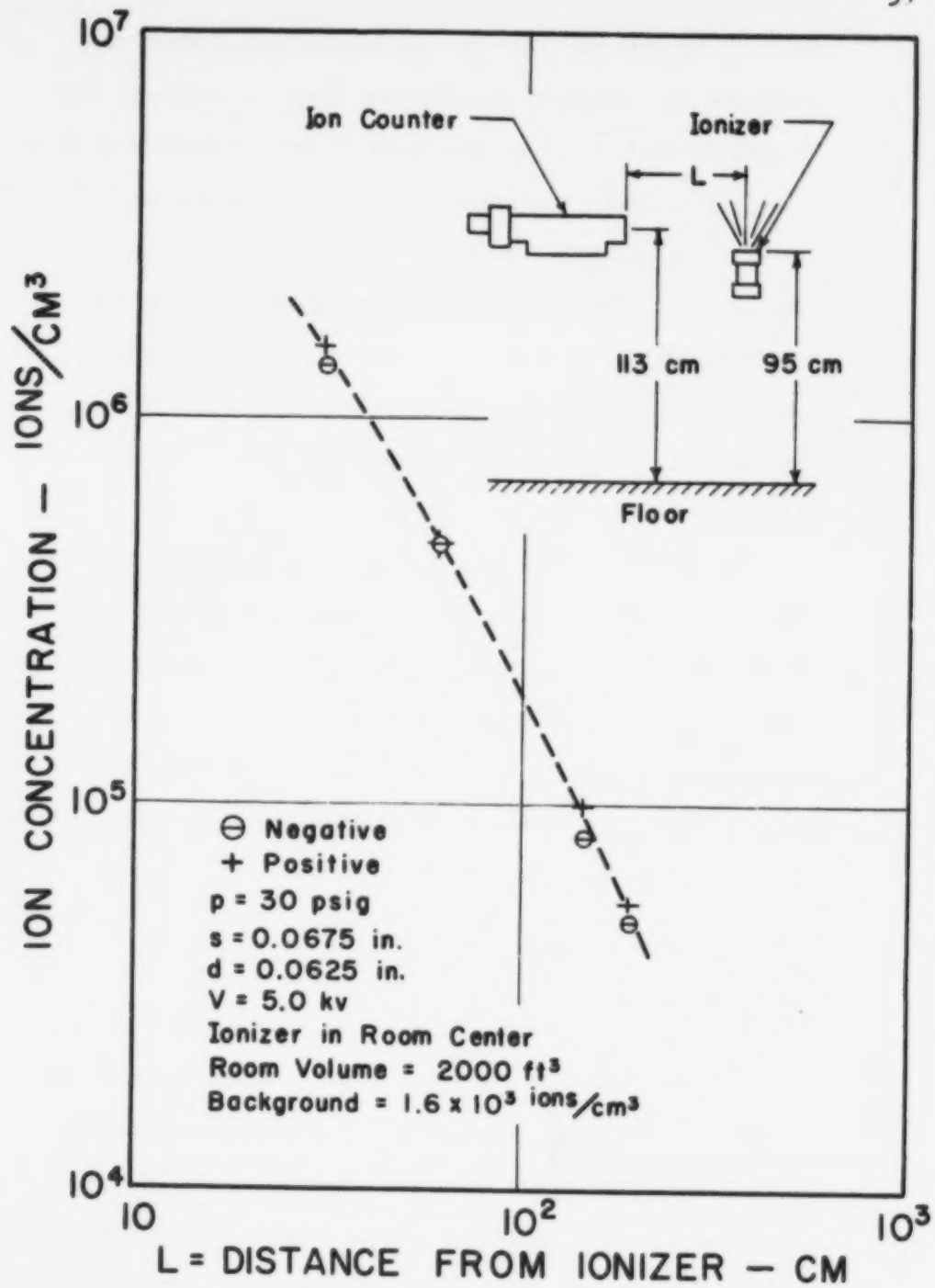

Figure 15 Unipolar ion concentrations measured perpendicular to the jet axis

It is apparent that the ion concentration drops off about as the square of the distance from the ionizer. The slight curvature of the line above an ion concentration of 10^5 ions per c.c. is probably caused by space charge precipitation on the charged plates of the ion collector. The measured concentration at 30 cm. should probably be doubled. Figure 15 does show, however, that it would be practically impossible to maintain a uniform, but high ion concentration in a room using a reasonable number of ion generators.

3. Time decay of ion concentration in a room. A few experiments were made in the room described above in which the unipolar ion concentration 60 cm. from the ionizer was measured after the ionizer power was turned off. Typical data is shown in Figure 16 along with the theoretical decay curves computed from equation 2 modified to include the background level:

$$n = \frac{n_o}{4\pi n_o e Z t + 1} + n_b \qquad (17)$$

where:

n_b = background concentration - ions/cm^3

It will be noted that the experimental concentrations after about 20 seconds are considerably higher than the theory. This hump in the decay curve was observed in all of the experimental data including several runs in a much larger room. The hump may be connected to the equalization of the ion concentration after the ion generator is turned off, or it may indicate a change in ion mobility as the

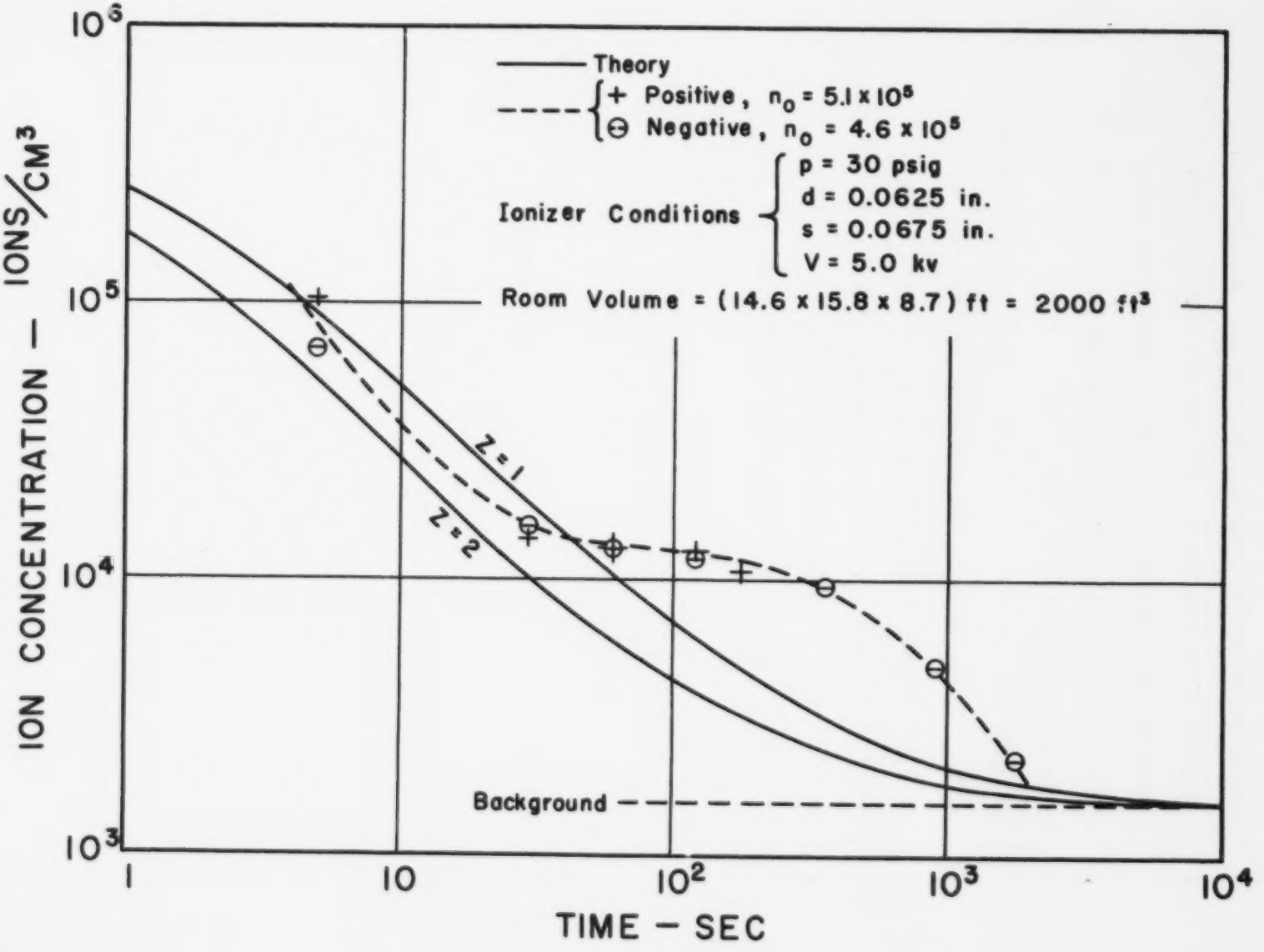

Figure 16 Decay of unipolar ion concentrations in a closed room

ions grow larger. However, it can be seen that the theory and experimental measurements are generally in agreement. Equation 17 is probably satisfactory for estimating the decay of ion concentrations in rooms, ventilating ducts, tubing, etc., wherever the time since generation and the initial concentration are known. In general the ion decay rate in rooms, ducts, etc. is independent of the geometry or size of the room and for strong ion sources such as the jet ionizer is also independent of the initial concentration. These remarkable characteristics of the decay process make it necessary to generate the ions as near as possible to the point where they are desired.

REFERENCES

1. T. L. Martin, "Climate Control through Ionization," J. Franklin Institute 254:267 (1952)
2. T. L. Martin, "Production of Unipolar Air with Radium Isotopes," AIEE Transactions J. Vol. 72 Part I, pp. 771-776 (1953)
3. W. W. Hicks and J. C. Beckett, "The Control of Air Ionization and Its Biological Effects," AIEE Trans. Vol. 76 Part I, pp. 108 (1957)
4. C. P. Yaglou, L. C. Benjamin, A. D. Brandt, "Physiological Changes During Exposure to Ionizer Air," Heating Piping and Air Contitioning 5:422-430 (1933)
5. G. Francis, "Ionization Phenomena in Gases," Academic Press (1959)
6. Instruction Manual Mark IV Ion Collector, Wesix Electric Heater Co., San Francisco 5, California
7. I. B. Wilson, "The Deposition of Charged Particles in Tubes, with Reference to The Retention of Therapeutic Aerosols in The Human Lung," J. Coll. Sci. 2:771-776 (1947)
8. W. W. Foster, "Deposition of Unipolar Charged Aerosol Particles by Mutual Repulsion," Brit. J. Appl. Phys. 10:206-213 (1959)
9. P. L. Magill, F. R. Holden and C. Akcley, "Air Pollution Handbook," McGraw Hill, New York (1956)
10. J. Townsend, "Application of Diffusion to Conducting Gases," Phil. Mag 45:471 (1898)
11. G. W. Penney and G. W. Hewitt, "Electrically Charged Dust in Rooms," AIEE Transactions 68:278-82 (1947)

APPENDIX A: ELECTRICAL CONVERSION UNITS AND NOMENCLATURE

1. Units

Practical	Electrostatic Units
1 volt	$\frac{1}{300}$ stat volt
1 coulomb	3×10^9 stat coulombs
1 ampere	3×10^9 stat coulombs/sec
1 electron charge	4.8×10^{-10} stat coulombs

2. Equations

A. Ion current to ion concentration

$$n = \frac{0.625 \times 10^{19} I}{Q} \qquad \text{(A-1)}$$

where:

I = ion current - amperes

Q = gas flow thru ionizer - cm^3/sec

n = free ions per cm^3

B. Ion current to ion output

$$N = 0.625 \times 10^{19} I \qquad \text{(A-2)}$$

where:

N = ions output - ions/sec

3. Nomenclature

a = characteristic linear dimension (cm)

b = constant (cm^2/sec)

d = orifice diameter (cm or inches)

e = particle charge (stat coulombs)

f,g,h = arbitrary functions

$\hat{i}, \hat{j}, \hat{k}$ = unit vectors in x,y,z directions

n = number concentration of charged particles (particles/cm^3)

n_b = background ion concentration (ions/cm^3)

n_o = initial concentration of charged particles (particles/cm^3)

q = volume generation of ions (ions/cm^3-sec)

r = radial coordinate in spherical or cylindrical geometries (cm)

t = time (sec)

u = particle velocity (cm/sec)

v = air velocity (cm/sec)

x,y,z = linear coordinates (cm)

A = area (cm^2)

E = electric intensity (stat volts/cm)

F_D = resistance force (dynes)

F_e = ponderomotive electrical force (dynes)

I = current (amperes)

L = length (cm)

N = total number of ions leaving generator (ions/sec)

P = pressure (psig)

Q = gas flow rate (cm^3/sec)

S = needle to orifice spacing (cm)

U = velocity along jet axis (cm/sec)

V = volume (cm^3)

Z' = particle mobility $\left(\frac{\text{cm/sec}}{\text{dyne}}\right)$

Z = ion mobility = $\frac{Z'}{e}$ $\left(\frac{\text{cm/sec}}{\text{stat volt/cm}}\right)$

α = recombination rate (cm^3/sec)

η = ionizer efficiency

ρ_e = charge density (stat coul/cm^3)

$\nabla = \hat{i}\frac{\partial}{\partial x} + \hat{j}\frac{\partial}{\partial y} + \hat{k}\frac{\partial}{\partial z}$

APPENDIX B

Self-Deposition of a Uniformly Charged Homogeneously Sized Aerosol or Unipolar Ions in the Absence of External Force Fields.

Summary

An equation for the self-deposition of ions and particulate matter on the boundaries of the system is developed for the cases of a uniformly charged homogeneously sized aerosol and unipolar ions in the absence of any external force fields. Only the electrical repulsive force between the charged particles is considered. The concentration decay equation is derived for one-dimensional rectangular, cylindrical, and spherical boundary configurations. The resulting decay equations are identical for the geometries considered.

B.1 Introduction

The problem to be considered here is: given a grounded, confined space in which there exists an initially uniform concentration of ions (or a uniformly charged homogeneously sized aerosol), what is the decay of concentration in the space due to the mutual repulsion of electrical forces acting between the particles?

An example of this type of problem is in the deposition of atmospheric dust upon the walls of a room. Atmospheric dust in buildings often carries a net charge. The mutual

repulsion of the charged particles causes some to migrate to the boundaries of the space (walls). Of course, in this example such factors as diffusion, impaction, and thermal migration may govern the deposition rate rather than the repulsive electrical forces.

Another example where this type of problem appears is in the decay of ion concentration in a closed space. In this report, two examples are mentioned: (1) the decay of ion concentration in a room and (2) the decay of ion concentration along a collector tube with no impressed electrical field. The first example is considered and worked out in the main body of this report, (Section V.B.3.), and a numerical example of the second application is worked out in this appendix, (Section B.6).

Analysis of the mutual repulsion type phenomenon are reported in the literature. J. Townsend (10) in his paper on diffusion in conducting gases considered the decay of charged density for the rectangular case when the number of (+) and (-) charges are not equal. Wilson (7) in his work on the deposition of particles in the human lung derived the decay equation based upon the assumption that the particle concentration is not a function of the linear coordinate of the system (it turns out such in this case). Penney and Hewitt (11) considered and determined the space charge potential created when single signed charged particles of uniform and constant concentration escape inefficient electronic air cleaners. W. W. Foster (8) considered

the deposition of an aerosol from a turbulent atmosphere in which he also assumed the concentration throughout the system is uniform at any given time. In the following derivation, this restriction will be removed and both ions and particles will be considered. The difference being accounted for in terms of their mobilities.

B.2 Derivation of the Governing Equation in One-Dimensional Rectangular Coordinates

Suppose that the uniformly charged homogeneously sized aerosol or ion system (which will be referred to as the charged particles hereafter) is placed between two grounded parallel infinite plates separated by a distance $2a$. Suppose further that it is possible to mix the charged particles so that at some initial time t_o the particle concentration n_o is uniform throughout the space between the two parallel plates. See Figure B-1.

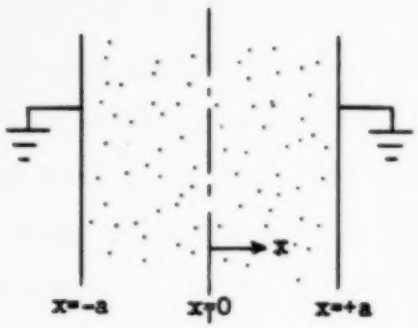

Figure B-1 One dimensional rectangular system

It is well known that there is a mutual repulsive force between the like charged particles, and that this repulsion will cause a net migration of particles to the grounded boundaries.

It is the purpose of this section to determine analytically the rate of decay of concentration within the enclosed space.

For a quasi-static space charge in a gas with unity dielectric constant and having a charge density of ρ_e Poisson's equation states:

$$\nabla \cdot \vec{E} = 4\pi \rho_e \qquad \text{(B-1)}$$

where:

$\vec{E}$ = electric intensity

$= \hat{i} E_x + \hat{j} E_y + \hat{k} E_z$ (stat volts/cm)

$\hat{i}, \hat{j}, \hat{k}$ = unit vectors in x, y, and z directions

$\nabla = \hat{i} \frac{\partial}{\partial x} + \hat{j} \frac{\partial}{\partial y} + \hat{k} \frac{\partial}{\partial z}$

ρ_e = charge density (stat coul/cm^3)

If the concentration of charged particles is n (particles/cm^3) with each particle having a charge of e (stat coul) and only the x-dimension is considered, equation B-1 may be written as:

$$\frac{\partial E}{\partial x} = 4\pi n e \qquad \text{(B-2)}$$

Each particle is acted upon by two forces. The first is the ponderomotive electrical force given by:

$$F_{ex} = e E_x \qquad \text{(B-3)}$$

The second force is the opposed resistance force given by:

$$F_{dx} = \frac{u}{Z'} \qquad \text{(B-4)}$$

where:

u = particle velocity in x-direction (cm/sec)

Z' = particle mobility (cm/sec per dyne)

In the absence of any external force fields (as gravitational, electrical, magnetic, etc.) these two forces are colinear

and opposite in direction. Neglecting acceleration effects allows the two forces to be equated, or:

$$E_x e = \frac{u}{Z'} \qquad \text{(B-5)}$$

Next consider an element of volume dV of the enclosed space with cross sectional area dA and length dx located somewhere between x = 0 and x = a (because of the symmetry of the problem only the positive x-direction need be considered).

The number of particles entering dA in an elemental time dt at x is:

$$n\ dA\ u\ dt$$

At x + dx, the number of particles leaving through dA in dt is:

$$n\ dA\ u\ dt + \frac{\partial}{\partial x}(n\ dA\ u\ dt)dx$$

Thus, the net number gain of particles by the volume in dt is:

$$-\frac{\partial}{\partial x}(nu)\ dx\ dA\ dt$$

But, the number gain of dV in dt is also:

$$\frac{\partial n}{\partial t}\ dV\ dt$$

Equating the two expressions gives:

$$\frac{\partial n}{\partial t} = -\frac{\partial}{\partial x}(nu) \qquad \text{(B-6)}$$

Replacing u in equation B-6 by its equivalent in equation B-5 gives:

$$\frac{\partial n}{\partial t} = -e\ Z'\ \frac{\partial}{\partial x}(nE) \qquad \text{(B-7)}$$

n and E are also related by equation B-2. Combining equations B-2 and B-7 and elminating n and its derivatives results in:

$$\frac{\partial^2 E}{\partial x\, \partial t} = -e\, Z' \frac{}{x} \left[E \frac{E}{x} \right] \qquad \text{(B-8)}$$

Equation B-8 may be integrated over x immediately:

$$\frac{\partial E}{\partial t} = -e\, Z' \left[E \frac{\partial E}{\partial x} \right] + f(t) \qquad \text{(B-9)}$$

where:

$f(t)$ is an arbitrary function involving possibly t but not x.

Next it will be shown that $f(t) = 0$. Due to the symmetry of the problem there is no net force upon the particles at $x = 0$. This implies that $E_{x=0} = 0$ (see equation B-3). Also, at $x = 0$ equation B-2 shows:

$$\frac{\partial E}{\partial x}\Big|_{x=0} = 4\pi e\, n\,(0,t) \leq 4\pi e\, n_0 = \text{constant}$$

Thus, it follows that:

$$\lim_{x \to 0} E \frac{\partial E}{\partial x} = 0$$

since $E \to 0$ and $\frac{\partial E}{\partial x} \leq$ constant as $x \to 0$.

Also since $E = 0$ at $x = 0$ for all time:

$$\frac{\partial E}{\partial t}\Big|_{x=0} = 0$$

Therefore, in equation B-9, $f(t) = 0$.

Equation B-9 thus becomes:

$$\frac{\partial E}{\partial t} = -e\, Z' \left[E \frac{\partial E}{\partial x} \right] \qquad \text{(B-10)}$$

The general solution of equation B-10 is:

$$x = e\, Z'\, E\, t + g \qquad \text{(B-11)}$$

Now at $t = 0$ equation (B-2) shows:

$$E(0,0) = 4\pi e\, n_0\, x$$

Using this condition, equation B-11 shows:

$$g = \frac{E}{4\pi e n_o}$$

Thus:

$$x = e Z' E t + \frac{E}{4\pi e n_o}$$

or:

$$E = \frac{x}{e Z' t + \frac{1}{4\pi e n_o}} \qquad (B-12)$$

Since $\frac{\partial E}{\partial x} = 4\pi e n$ or $n = \frac{1}{4\pi e} \frac{\partial E}{\partial x}$ equation B-12 may be solved upon differentiating for $n(x,t)$, or:

$$n = \frac{n_o}{4\pi e^2 n_o Z' t + 1} \qquad (B-13)$$

Equation B-13 is the result which has been sought. It is interesting to note that n depends upon neither the variable x nor upon the characteristic dimension of the system a. Thus the concentration between the two plates remains uniform although the level decreases with time.

B.3 Solution in Cylindrical Coordinates

Suppose the boundary of the space is a grounded infinitely long cylinder of radius a. Using the same approach as in the rectangular case it is possible to develope the concentration decay equation for the cylindrical system.

In cylindrical coordinates the Poisson equation is:

$$\frac{1}{r} \frac{\partial}{\partial r} (rE) = 4\pi e n \qquad (B-14)$$

where:

r = radial coordinate (cm)

A force balance in the radial direction gives:

$$eE_r = \frac{u_r}{Z'} \qquad (B-15)$$

The number balance of equation B-6 may be rederived in cylindrical coordinates to give:

$$\frac{\partial n}{\partial t} = -\frac{1}{r}\frac{\partial}{\partial r}[r\, n\, u] \qquad \text{(B-16)}$$

In precisely the same manner as in the preceding section, equations B-14, B-15 and B-16 may be combined to yield:

$$\frac{\partial^2(rE)}{\partial r\,\partial t} = -e\, Z'\frac{\partial}{\partial r}\left[E\frac{\partial}{\partial r}(rE)\right] \qquad \text{(B-17)}$$

Equation B-17 may be integrated over r to give:

$$\frac{\partial}{\partial t}(rE) = -e\, Z'\, E\frac{\partial}{\partial r}(rE) + g(t) \qquad \text{(B-18)}$$

By employing the same line of reasoning as used in the rectangular case, it may be shown that $g(t) = 0$. Equation B-18 becomes:

$$\frac{\partial}{\partial t}(rE) = -e\, Z'\, E\frac{\partial}{\partial r}(rE) \qquad \text{(B-19)}$$

The solution of which is:

$$r = e\, Z'\, E\, t + h \qquad \text{(B-20)}$$

Now, at $t = 0$ equation B-14 shows:

$$r_{t=0} = \frac{E}{2\pi\, e\, n_o}$$

Thus:

$$r = E\left[e\, Z'\, t + \frac{1}{2\pi\, e\, n_o}\right] \qquad \text{(B-21)}$$

or:

$$E = \frac{r}{e\, Z'\, t + \frac{1}{2\pi\, e\, n_o}} \qquad \text{(B-22)}$$

Again, the particle concentration is given by equation B-14:

$$n = \frac{1}{4\pi\, e\, r}\frac{\partial}{\partial r}(rE)$$

or, combining equations B-14 and B-22:

$$n = \frac{n_o}{4\pi e^2 Z' n_o t + 1} \qquad \text{(B-23)}$$

Thus, for a cylindrical geometry n is independent of the radius and of the size of the system. Indeed, the result is precisely the same as that of the rectangular case.

B.4 Solution in Spherical Coordinates

Following the same development as in the two previous sections the pertinent basic equations are

Poisson's equation:

$$\frac{1}{r^2} \frac{\partial}{\partial r} (r^2 E) = 4\pi e n \qquad \text{(B-24)}$$

the force balance equation:

$$eE = \frac{u_r}{Z'} \qquad \text{(B-25)}$$

and the number conservation equation:

$$\frac{\partial n}{\partial t} = - \frac{1}{r^2} \frac{\partial}{\partial r} (r^2 n u) \qquad \text{(B-26)}$$

From these three equations plus the initial condition considerations, it may be shown that:

$$E = \frac{r}{3e Z' t + \frac{3}{4\pi e n_o}} \qquad \text{(B-27)}$$

or:

$$n = \frac{n_o}{4\pi e^2 Z' n_o t + 1} \qquad \text{(B-28)}$$

Again, the result is the same as for the rectilinear and cylindrical cases. This result is not suprising since the concentration is neither a function of the linear variable

nor of the size of the system. In summary, the concentration is independent of the system geometry for those cases considered.

B.5 Application to Unipolar Ions

The derived deposition equation:

$$n = \frac{n_o}{4\pi e^2 Z' n_o t + 1}$$

may be modified somewhat for ease in working with unipolar ions.

Define:

$$Z = \frac{Z'}{e} \qquad \text{(B-29)}$$

Then the deposition equation becomes:

$$n = \frac{n_o}{4\pi e Z n_o t + 1} \qquad \text{(B-30)}$$

Using a value of $e = 4.8 \times 10^{-10}$ stat coulomb and a value of $Z = 600 \frac{\text{cm/sec}}{\text{stat volt/cm}}$ (which is a reasonable figure for small ions) allows equation B-30 to be written:

$$n = \frac{n_o}{3.61 \times 10^{-6} n_o t + 1} \qquad \text{(B-31)}$$

B.6 Example: Decay of Ion Concentration in a Grounded Collector Tube

In Appendix section B.1 it was mentioned that a 2 cm I.D. copper tube was used to collect the ions produced by the ionizer. It will be shown here that this method of collection is an efficient one. Assume a typical operating condition of

2.4 cfm (1130 cm^3/sec) of air flow through the ionizer with an ion current of 7.5×10^{-6} amperes.

The air velocity through the tube is:

$$v = \frac{Q}{A} = 360 \text{ cm/sec}$$

Since the tube is 60 cm long, an element of air resides in the tube for a time:

$$t = \frac{\text{length}}{\text{velocity}} = \frac{60}{360} = \frac{1}{6} \text{ sec}$$

An ion current of 7.5×10^{-6} amperes is equivalent to the production of 4.7×10^{13} ions/sec, or:

$$n_o = \frac{4.7 \times 10^{13}}{Q} \text{ ions/sec} = 4.14 \times 10^{10} \text{ ions/cm}^3$$

Using these results in equation B-31 gives:

$$n = \frac{n_o}{1.5 \times 10^5 \, t + 1}$$

or, for $t = 1/6$ sec:

$$\frac{n}{n_o} = \frac{1}{4} \times 10^{-5}$$

So for this example, for every one million ions entering the collection tube roughly two escape.